Detection and Dissolution of Needle-like Hydroxyapatite Nanomaterials in Infant Formula

Jared J. Schoepf[1], Yuqiang Bi[1], Justin Kidd[1], Pierre Herckes[2], Kiril Hristovski[1], Paul Westerhoff[1]*

* Corresponding Author: p.westerhoff@asu.edu; 480-965-2885;

1- Arizona State University, School of Sustainable Engineering and The Built Environment, Box 3005, Tempe, AZ 85287-3005

2- Arizona State University, School of Molecular Sciences, Box 1604, Tempe, AZ 85287-1604

Date of Last Revision: December 12, 2016

In preparation for Submission to: *NanoImpact*

ABSTRACT

The unknowns surrounding presence, composition and transformations during the use phase of engineered nanoparticles (ENPs) in consumer products raises potential human and environmental health concerns and public discourse. This research developed evidence and confirmatory analytical methods to determine the presence and composition of ENPs in a consumer product with a complex organic matrix (six different infant formula samples). Nano-scale crystalline needle-shaped hydroxyapatite (HA; appx. 25 nm x 150 nm) primary particles, present as aggregates (0.3-2 μm), were detected in half the samples. This is the first report of these ENPs in infant formula. Dissolution experiments with needle-shaped HA were conducted to assess potential transformations of nano-HA particles. Rapid dissolution of needle-shaped HA occurred only under lower pH conditions present in simulated biological fluids (acidic gastric fluids), but not in simulated drinking water (near-neutral pH). Other non-nanosized HA minerals exhibited less dissolution under the same low pH conditions. This work demonstrates the occurrence of engineered nanomaterials in the food supply of a sensitive population (infants) and the need to consider transformations in nanomaterials that occur during use, which result in different exposures between pristine/as-produced ENPs and nanomaterials after passing through the human gut.

Keywords: nanomaterials, calcium phosphate, water, digestion

1. INTRODUCTION

Many minerals exist in both natural and engineered nanoparticle (ENP) forms. While the occurrence of naturally occurring nanoparticles (e.g., hematite, hydroxyapatite) is well recognized in natural systems, the environmental behavior of ENPs raises new regulatory and health concerns. These concerns primarily stem from existing knowledge gaps in understanding the ENP risks, which could be summarized in two categories: (1) discovering where ENPs are used in commerce and hence might enter the environment, and (2) elucidating ENP transformations from pristine materials, to synthesis in the lab or factory, and through use and end-of-life phases. We and others have previously shown that silicon- and titanium-oxide ENPs exist in foods, are ingested by humans, and pass through wastewater treatment plants, which results in their release to surface waters and terrestrial systems where sewage solids are land applied [1-8]. These two ENPs undergo little dissolution (i.e., transformation) during this process, which differs from antimicrobials like silver, copper, or zinc nanomaterials [9-12].

Calcium phosphate minerals are an example of solids present in nature and used in environmental remediation/treatment processes [13-18] or human nutritional supplements. Intentional formation of calcium phosphate is used to immobilize heavy metals in soil [19, 20], remove fluoride from water to protect public health, [21] or remove phosphate from wastewaters to limit the eutrophication potential of wastewater discharges [17]. Calcium phosphate, also referred as tricalcium phosphate (TCP), is used as a leavening agent in foods, a polishing material in toothpaste, an antioxidant activity promoter and texture stabilizer in canned vegetables, a firming agent or to avoid formation of clumps in food. Hydroxyapatite (HA; $Ca_5(PO_4)_3$ or $Ca_5(PO_4)_3(OH)$) is a common form of calcium phosphate. Many people take calcium supplements, including calcium carbonate, calcium citrate and hydroxyapatite forms, but

the literature is mixed on which form leads to greater bioavailable calcium for health bone development [22, 23]. In other applications, nano-forms of calcium minerals have raised concern. For example, the European Union Scientific Committee on Consumer Safety 2015 opinion on nano-HA states that the safety of its use in oral and cosmetic products cannot be currently decided due to limitations in available data, including the exact size, shape and crystallinity of the nano-HA, but that the available information indicates nano-HA in needle form is potentially toxic when used in dermally-applied cosmetic products [24].

Calcium is an essential element for all biological organisms, and is widely used in human food supplements. For example, infant formula is intended to be the sole nutrition source for infants for the first 12 months. Although regulations (e.g. 21 CFR 107.100 in the USA) stipulate the elements required in the infant formula, they lack guidance on the type or size of the compounds used to provide the nutrients. Regulations refer to HA as generally regarded as safe (GRAS); however, new bottom up manufacturing processes that create nanomaterials compared to top down processes create new concerns if the GRAS status applies. Given potential toxicity concerns raised in the EU on nano-needle-shaped hydroxyapatite in products intended for human use, the need for infants to have calcium and other elements (P, Fe) in their diets, and potential transformations for HA under different pH conditions, we undertook a study to separate and identify HA and other nanomaterials in powdered infant formulas. This challenging work with infant formulas that contain salts, sparingly soluble minerals, fats and other components is a precursor to understanding the occurrence and role of nano-scale HA minerals in complex environmental matrices (soil, biota, and water).

To identify initially unknown nanomaterials in infant formula, samples were separated by centrifugation after dispersing powders in water and then analyzed by transmission electron

microscopy (TEM) with energy dispersive X-ray spectroscopy (EDS) and X-ray diffraction (XRD). Findings from these samples were compared against reference calcium phosphate materials. We focused on HA because it was found in three out of six samples, although it has not yet been widely considered by the health and safety exposure community as a risk in the food supply system. Within a complex food matrix, HA nanoparticles are difficult to be detected using conventional analytical paradigms. A secondary focus was the dissolution of HA in synthetic biological fluids to explore potential transformation in human body of these nano- and micron-sized minerals. Because the intended function of calcium phosphate in infant formula is to promote nutrient uptake, we used aqueous matrices representing simple drinking water and simulated gastric fluids. Understanding nanomaterial transformations during their intended use emerges as a critical discussion and conclusion point around the benefits of using nanotechnology (e.g., rapid dissolution of HA to deliver calcium and phosphate ions).

2.0 MATERIALS AND METHODS

2.1 Chemicals

Six infant formulas from different companies (Gerber, Similac, Enfamil, and Well Beginnings) were purchased in the United States and identified, for confidentiality, as S1-S6. Samples S1-S5 were dry powders, and S6 was a liquid concentrate. Dry powders and a liquid concentrate were chosen to compare suspected different additives used for each product. Three reference powder samples of food-grade calcium phosphate, labeled as hydroxyapatite, were procured from three different vendors. Samples R1 (American Elemental) and R2 (Hebei Shunye Import and Export Limited Company) were labeled as 99% pure and containing needle-like

nano-HA. Sample R3 (NOW Foods) was an HA supplement provided in a gelatin pill capsule; only the contents of an opened capsule were used in analysis and dissolution tests.

2.2 Electron Microscopy Analysis

Infant formula (0.15 grams) samples S1-6 and HA reference samples R1-3 were suspended in 40 mL ultrapure water (18.2 MΩ cm, Nanopure Infinity, Barnstead) and sonicated (80 Watts/L, Branson Ultrasonic Bath, Emerson) for 30 minutes to disperse particles. This mass to liquid ratio was used to parallel work other food samples analyzed by our group [25, 26]. Additional electron microscopy experiments were conducted at solid to liquid ratios based upon recommended sample preparation on the infant formula packaging, and showed no dependence of outcomes on solid to liquid ratios. Other detailed control and validation experiments are summarized in Table SI.4 and described in the results section.

Step-by-step description of sample preparation of electron microscopy samples are summarized in Figures SI.2 through SI.5. Briefly, samples in 50 mL vials were centrifuged at *F* =14,000 G for 15 minutes. The organics-rich supernatant was poured off, leaving a pellet of particulate matter at the bottom of the centrifuge tube. The pellet was re-suspended in 20 mL ultrapure water and inverted by hand for 30 seconds, then 50 µL volumes were pipetted onto a copper/lacey carbon transmission electron microscopy (TEM) grid and allowed to air-dry overnight. Microscopy was performed on a Philips CM200 HR-TEM with energy dispersive X-ray spectroscopy (EDS). To confirm HA was not an artifact from sample preparation, a pure powder reference sample of HA was procured, deposited on a SEM stub (Figure SI.3) and directly analyzed as a powder by scanning electron microscopy (SEM; FEG XL30 ESEM with EDS system) with energy dispersive spectroscopy. Mean particle diameter, particle size

distributions, and cumulative distribution below 100 nm were determined by manually measuring the particles sizes of 250 particles from the images using ImageJ software and conducting statistical analysis.

2.3 Sample Preparation for Confirmation and Quantification of Hydroxyapatite

Figure SI.6 provides a step-by-step description of sample preparation. To determine the relative amount of hydroxyapatite nanoparticles in infant formula, 10 grams of each formula sample (six in total) was weighed into 50 mL centrifuge tubes with 40 mL of ultrapure water (18.2 MΩ cm, Nanopure Infinity, Barnstead). The mixed samples were then centrifuged for 20 min at F = 14,000 G to separate lighter components. The pellet collected at the bottom of centrifuges was washed three additional times with UP water. The washed pellet was freeze-dried under vacuum for 48 hours (FreeZone Freeze Dry System, Labconco), weighed, and compared with the weight of starting material to calculate the relative concentration of collected minerals. The mineral phases of pellets and reference powders were prepared (Figure SI.7) and analyzed using powder X-ray diffraction (pXRD) using a Siemens D5000 diffractometer with a monochromated Cu–Kα radiation at 40 kV and 30 mA. Each sample was scanned at 2θ values from 10° to 70° to collect diffractograms, which were compared with the diffraction patterns of standard materials in ICDD database.

2.4 Dissolution Experiments using Hydroxyapatite in Aqueous Media

Ultrapure water and simulated biological fluids were used to examine the dissolution potential of the two reference HA and calcium bioavailability after ingestion. A detailed procedure is outlined in Figure SI.1. A Fed-State Gastric Fluid (Fed-SGF, pH 5.0) and a Fasted-

State Gastric Fluid (Fast-SGF, pH ~ 1.6) were prepared following recipes reported previously [27] and detailed in Table SI.1. For HA dissolution, 40 mL of the media was placed in 50 mL plastic centrifuge vials followed by the addition of 8 mg of reference HA to achieve a final concentration of 200 mg/L. The HA concentration was chosen to represent the serving size of HA per serving of infant formula. Immediately after mixing HA with simulated media, the suspensions were placed on a rotational shaker (45 rpm). The fed-state gastric fluid and fasted-state gastric fluid were rotated for 2 hours to mimic the average contact time of food in the human stomach [27]. Within 5 minutes of the completion of mixing, 15 mL of each suspension was filtered through 30kDa centrifugal ultrafilters (NMWL=30K Da, ultracel regenerated cellulose, EMD Millipore) at F = 4,000 G for 12 minutes. A HA dose of 200 mg/L was added to the aqueous chemistry described in Table SI.1. The solution collected for each filtered sample was diluted in 2% nitric acid and analyzed for dissolved calcium and phosphorous concentrations by inductively coupled plasma mass spectrometry (ICP-MS, X-Series-II, Thermo Scientific).

Control experiments were performed to understand potential impact of matrix effects (DI water, 1 mM $NaHCO_3$, biological fluids) on permeation of dissolved Ca^{2+} through the ultrafilter or matrix effects due to calcium precipitation. Details and results provided in Supplemental Information (Table SI.2) concluded that there were no matrix effects in DI water, 1 mM $NaHCO_3$, or gastric fluids (pH 1.6 or 5.0), and >90% of the spiked Ca^{2+} was recovered.

2. RESULTS AND DISCUSSION

3.1 Presence of Nanomaterials in Powder Formulas

Detecting nanomaterials in complex matrices is a challenge [28-30]. Initially, powder formula samples were analyzed by scanning electron microscopy (SEM), but the amount of organic material prevented meaningful imaging from carbon contamination (see Table SI.4), the

deposition of carbonaceous material by the electron beam from cracking of carbon-carbon bonds present on the sample and carbon residual within the vacuum of the sampling chamber of the microscope [31]. To overcome these issues and achieve high quality TEM images and meaningful elemental analysis of solids, infant formula samples were added to water and then followed protocols described in the methods section. Results are discussed in two parts. First, the observed results show needle-like HA is present in some infant formula samples. Second, experiments demonstrate such structures are not artifacts of sample preparation.

TEM images in Figure 1 are representative of multiple (typically greater than 10) images taken across several TEM grids of each sample. All six infant formula samples contained Ca and P as determined by EDS (Table 1), suggesting the presence of Ca-containing minerals. In addition, SiO_2 nanoparticles were found to be present in one sample (S4) and had similar size (~ 7 nm) and shape with this nanomaterial in other foods [32]. Titanium and oxygen containing material was detected in the liquid formula (S6) and was consistent with TiO_2 nanomaterials in foods reported in the literature [25, 33]. Previous studies in food samples discuss occurrence and characterization of SiO_2 and TiO_2 materials [32-34], and therefore are not discussed further here.

The three most prevalent elements in colloids detected on the TEM grids were calcium, phosphorous and oxygen, and these were associated with the colloidal materials having two general shapes (needle-like or spherical). Figure SI.8 shows representative TEM with EDS spectra for these colloidal materials and additional TEM images of the samples. S1, S2, and S3 samples contained needle-like shaped particles 10-30 nm in width and 100-300 nm in length, creating impressions of dendritic networks. The size and shape of HA in S3 were nearly identical to the needle-like hydroxyapatite reference (R1 and R2) samples (Figure 1). Additional TEM of the three reference materials are shown in Figure SI.9. Samples R1 and R2 containing nearly

exclusively needle-like shaped HA whereas sample R3 contains only a few needle-like structures but mostly other micro-crystalline HA structures. This mineral phase, however, was not observed in S1 and S2, although TEM characterization suggested its presence.

XRD data for each sample and reference material are presented in Figure 2. Initial XRD performed on the entire powdered infant formula samples exhibited a broad peak due to all the salts and organic materials. Therefore, XRD analysis for the infant formula samples were conducted on a purified pellet (Figure 2 for S1-S6), but it was feasible to conduct XRD directly without sample pretreatment for the three reference HA. Figure SI.10 shows XRD diffraction pattern confirming the presence of a single phase hydroxyapatite ($Ca_5(PO_4)_3(OH)$) in the three reference materials. The two needle-like hydroxyapatite reference samples (R1 and R2) have sharper diffraction peaks compared to the spherical counterpart which contains only a few needle-like structures but mostly other micro-crystalline HA structures (R3), suggesting larger crystallite sizes of R1 and R2 than R3. The micro-crystalline R3 sample was found to have similar morphology within S5, both displaying spherical shapes. Of the six infant formula samples (S1-S6) in Figure 2, one or both forms of calcium was observed (calcite or calcium hydroxyapatite). XRD analysis unambiguously confirmed the presence of hydroxyapatite in S3 based upon library matches (Figure 2). Samples S5 appeared to be mostly calcium hydroxyapatite, whereas other samples appear to contain a mixture of calcite and calcium hydroxyapatite. In S5 sample, however, the calcium phosphate was dispersed in larger aggregates composed of organics and calcium material and mainly composed of monetite minerals ($CaHPO_4$) based upon XRD analysis.

Together, TEM and XRD analyses provide evidence that needle-shaped Ca-containing nanomaterials are present in 3 out of 6 infant formulas (S1, S2, and S3), likely in the form of HA

or HA/calcite mixture. To assess the quantity of nano-scale needle-like HA in the samples, materials were separated from the rest of formula constituents via repeated sonication, centrifugation, and washing (Figure SI.6). The minimum concentration of HA in S3 was estimated to be ~0.4 wt% based on the mass of insoluble pellet. The HA mass recovered in pellets from samples S1 and S6 was < 0.1 wt%, and even less mass was recovered from the other samples.

The presence of needle-like HA in the infant formula was unexpected. Therefore, an extensive array of experiments was performed using S3 and R1 to confirm their presence in the samples and demonstrate they were not artifacts of sample preparation. Complete details are provided in Supplemental Information text and summarized in Table SI.4. First, to assess the potential for artifacts or transformations in nanomaterial morphology and size experienced in sample preparation, hydroxyapatite reference materials were purchased and analyzed using the same sample preparation as the infant formulas (sonication, centrifugation, decantation, and resuspended (following steps in Figure SI.2). During the same sample preparation, the needle-like and spherical reference materials maintained their size and morphology through the process, concluding sample preparation did not alter the nanomaterials in the infant formula. SEM analysis directly on the infant formula powder was not able to detect needle-like HA because of the presence of salts and organics in the powder, where HA accounts for <0.4% of the dry mass of powder. Therefore, dispersion of the powder in water and separation of solids was necessary (see discussion related to Figures SI.12-17).

Second, the infant formula (S3) was prepare at a higher solids to liquid ratio (6 grams instead of 0.15 grams in 40 mL of water) to represent the recommend ratio to prepare the infant formula as described on the package label. The samples were mixed by hand but not sonicated.

Liquid was then either pipetted (20 mL) directly onto a TEM grid or centrifuged (4050 G for 4 hours) onto a TEM grid placed in the bottom of the centrifuge vial. In both cases, TEM analysis of the grids detected nano needle-like HA (Table SI.4). Thus, neither the solid-to-liquid ratio nor method of preparing the TEM grid lead to artifacts in needle-like HA detection.

Third, evidence exists that needle-like HA could form due to sonication [35-37]. To demonstrate that sonication did induce needle-like HA formation experiments on dispersed S3 were performed. Sample S3 was prepared for TEM analysis following our original method (Figure SI.2) that included sonication, compared against the sample procedure without sonication. Figure SI.11 shows nearly identical TEM images from these comparative experiments. Nano needle-like HA is present both with and without sonication. Thus, this confirms that sonication of the infant formula added to water under the conditions applied herein does not lead to artifacts related to needle-like HA formation. Upon further inspection of the literature on needle-like HA synthesis, conditions (sonication power of 300 watts for 3 hours and 333 ^{o}K) required to produce needle-like HA during sonication do not exist during our preparation of sample S3 (Figure SI.2 where sonication power 80 watts for 30 min and 300 ^{o}K).

Fourth, additional experiments were conducted to confirm our sample pretreatment did not in-situ produce needle-like HA due to the presence of dissolved calcium and phosphorous in the presence of other salts or organic macromolecules that might be present in infant formula. Sample S3 was dispersed in water and needle-like HA centrifuged out, into a pellet, following our original methodology. To the supernatant, absent of needle-like HA pellet, which still contains macromolecules and other inorganics, calcium and phosphorus ions were added to the supernatant at a 1.67 mole ratio (the optimum ratio for HA synthesis [36]) and then bath sonicated. Subsequent centrifugation and TEM inspection did not detect HA on the TEM grid.

Thus, neither sonication alone nor sonication in the presence of other inorganic/organic components present in the infant formulas could produce nano needle-like HA artifacts, under the sample preparation conditions used in our work.

3.2 Dissolution Potential for Hydroxyapatite as a Function of pH in Biologically Relevant Media

High surface area or high aspect ratio of nanomaterials can increase the rate of mineral dissolution and result in the release of soluble ions [11, 38-41]. While dissolution of nanomaterials can result in toxic responses for some metals (e.g., silver, zinc, copper) for other ENPs, we hypothesized that a beneficial reason of adding needle-like HA nanomaterials to the infant formula may be to increase dissolution potential of the mineral phase and bioavailability of calcium and phosphate. Therefore, dissolution experiments for the reference needle-like (R1) and spherical (R3) hydroxyapatite materials were conducted in simulated drinking waters and biological fluids. The dissolution potential of HA in each matrix was based upon permeation of calcium ion through the 30 kDa ultrafilter. The HA nanomaterials have larger radii than the pore size of 30kDa filters (~2 nm), allowing for the size exclusion of HA ions and colloidal HA [42]. Controlled experiments described in Supplemental Information confirm that matrix effects do not influence Ca^{2+} permeation across these ultrafilters under the operating conditions tested.

Figure 3 shows that dissolution of hydroxyapatite occurs in the two gastric fluids, while less than 6% of the HA dissolves in 1 mM $NaHCO_3$ and permeates the ultrafilters. In the pH 5.0 gastric fluid, more than 60% of needle-like HA (R1) and <50% of the spherical HA (R3) dissolves. At pH 1.6, similar levels of needle-like HA (R1) dissolution occurs but a higher amount of dissolution occurs for spherical HA (R3). Similar patterns in UF permeation of

phosphate during these tests were also observed (Figure SI.18). Visual observations during the experiments indicate more rapid changes for R1 than R3 samples. Both samples were white and cloudy initially, but R1 became clear in < 1 minute whereas the change in visibility took 1-2 hr for R3 (see supplemental information Figures SI.19-20). The two hour period is physiologically relevant for the contact time for food and acidic gastric fluids [27]. These visual observations may indicate disaggregation or dissolution. Measurement of dynamic light scattering after each dissolution test indicated a significant decrease in mean diameters for the needle-like HA reference material (Figure SI.19), which could indicate either disaggregation or dissolution. Overall, the quantitative data for calcium and phosphorous, as indicators of HA, presented in Figure 3 were supportive of qualitative visual observations.

Attempts were made to differentiate ionic from colloidal forms of Ca and P using single-particle ICP-MS, which is a powerful tool for analysis of many nanoparticles in aqueous media [7, 43-47]. However, the minimum detection of Ca and P elements and associated mineral forms were more than several hundred nanometers due to the response factors of the ICP-MS [28]. This highlights an important research need to improve sensitivity of spICP-MS for materials like HA.

Thermodynamic chemical equilibrium modeling (Visual MINTEQ (ver. 3.1)) predicts complete dissolution of HA in either gastric fluid (Figure SI.22). The discrepancies between model predictions and experimental observations (Figure 3) indicate that the dissolution of HA in the simulated gastric fluids may have kinetic limitations or differences in solubility products for different aspect ratio HA or presence of non-crystalline forms of calcium phosphate solids. In comparison to two other calcium minerals (i.e., calcite, monetite) identified in infant formula, hydroxyapatite has the lowest solubility at pH > 5.4 (Figure SI.22). However, in both gastric

316 fluids, all calcium minerals are predicted to dissolve completely at equilibrium with a serving
317 concentration of 2 mM Ca in infant formula. Future research is needed to quantify the rates of
318 dissolution for these two different HA morphologies.
319 The calcium bioavailability of different minerals cannot be concluded until additional
320 kinetic studies are performed. However, the comparison between R1 (needle-like) and R3
321 (spherical) samples of HA (confirmed by XRD) suggest a priori assumptions about
322 thermodynamic stability constants may not be appropriate for different shapes of HA. The
323 dissolution mechanisms of calcium phosphate nanomaterials with respect to shape are not well
324 understood. However, dissolution of high aspect ratio (i.e. needle-shaped) metal oxide
325 nanoparticles have been reported to dissolve preferentially from each of the two ends [48].
326 Numerous methodologies exist to synthesize calcium phosphate, including those to produce
327 needle-like nanostructures [35, 36], and it appears these different shapes could impact ability to
328 dissolve in the acid biological fluids.
329 **Human Exposure Impact of Findings**
330 TEM detected the presence of nanoparticles in all six samples. Results show that
331 hydroxyapatite was detected in multiple samples at levels on the order of <0.1 to ~0.4 wt%.
332 Other samples contained calcite, monetite, silica dioxide, and titanium dioxide at lower levels.
333 Most attention was placed on hydroxyapatite because the presence of calcium nanomaterials in
334 infant formula has not been reported previously. In the authors opinion, hydroxyapatite (needle-
335 like structure) may be intentionally used in infant formula because of its rapid (almost
336 instantaneous) dissolution potential in gastric fluids at and below pH 5. However, further
337 research is needed to prove this hypothesis. Previous research suggests hydroxyapatite
338 dissolution provides favorable stoichiometric ratios of bioavailable Ca and P [49-51]. Slower

dissolution of spherical hydroxyapatite may not provide as much nutritional benefit. Additional techniques are needed to measure needle-like particles as FFF-ICP-MS, and spICP-MS measure particle size, but not morphology resulting in difficulty interpreting results for needle-like materials.

Others have reported the global production of many types of ENMs, yet these reports exclude needle-like hydroxyapatite [16, 52, 53] while one report quantifies the amount of HA in the USA entering the environment from the use in toothpaste to be between 18 and 19 metric tons per year in 2013 [54]. The 2013 global market for infant formula was approximately $41 Billion (US dollar), and growing rapidly in Asia and other markets [55]. Based upon the prevalence of the material in infant formula alone, the global annual production is likely to be on the order of carbon nanotubes, in the range of thousands of metric tons per year (see Supplemental Information).

The dissolution potential of needle-like HA under mildly acidic conditions raises a number of issues for assessing the impact of these types of nanomaterials. First, the US EPA Toxic Substances Control Act (Section 8 rule for nanomaterials) may exclude, from being classified as nanomaterials, substances which dissociate completely in water. The needle-like HA examined here would be difficult to classify, because it did not rapidly dissolve in water at near neutral pH, but did dissolve rapidly under mildly acidic conditions where it was intended to be used (i.e., digestive tract). Further proposed rule changes would exclude substances from being classified as nanomaterials which do not exhibit new properties when their size falls in the range of 1-100 nm. For HA it appears that the needle-like shape is intended to increase the rate of dissolution in acidic conditions, and this needle-like structure is specifically synthesized by controlled chemical and heating conditions through a new bottom up manufacturing process

compared to standard top down processes. Therefore, needle-like HA could pose a challenge to proposed classification systems under this rule for ENPs in the USA.

Second, evaluating the toxicity in mammalian cell culture of needle-like hydroxyapatite may give very different results from *in vivo* administration, where acidic conditions in gastro-intestinal tracts would apparently rapidly transform (i.e., dissolution) the size of this HA engineered nanoparticle. Calcium ions are absorbed by the small intestine by passive diffusion and active transport [56, 57], but recrystallization of HA may occur. If there is a high concentration of phosphate and calcium ions in the small intestine under alkaline conditions, you can get precipitation of HA [58]. This could impact the effects of HA on the gut microbiome because they would be exposed to non-dissolved (i.e., near pristine) forms of the ENP. Thus working with ENPs like needle-like HA raises challenges to appropriately track dosimetry throughout toxicological testing [59-61].

Finally, elements in other nanomaterials (silver, copper, zinc, cadmium, etc.) can dissolve out of nanomaterials based upon variable environmental conditions. Whereas redox conditions in solution can control the ionic release (Ag^{+}, Cu^{2+}, Zn^{2+}, etc.) from these ENPs, dissolution of calcium and phosphate ions from HA appears to be controlled by its pH-dependent solubility rather than redox conditions in water. The needle-like HA structure may have different K_{SP} values compared against other calcium phosphate forms, or may just influence the relative dissolution kinetics. Fortunately, calcium and phosphorous are not toxic like other metals.

ACKNOWLEDGEMENTS

Funding was provided from the US Environmental Protection Agency through the STAR program (RD83558001) and the National Science Foundation through the Nano-Enabled Water

Treatment Technologies Nanosystems Engineering Research Center (EEC-1449500) and CBET 1336542. Assistance from Ian Illuminati from Friends of the Earth is appreciated. We gratefully acknowledge the use of the facilities within the LeRoy Eyring Center for Solid State Science at Arizona State University.

390 Table 1 – Sample and reference material characteristics from label information, TEM/SEM*, and

391 EDS**.

Sample ID	Manufacturer Brand / Product ID #				
	Product & Label Information	**Elements detected****	**Likely nano-scale minerals / elements**	**Dimension of primary particles***	**Dimension of aggregates***
S1	*Powder formula* (120 mgCa; 66 mgP; 1.8 mgFe)	Ca, P, O	Nano needle-like HA	13nm (width) by 110nm (length)	320 – 1,627 nm
S2	*Powder formula* (82 mgCa; 44 mgP; 1.9 mgFe)	Ca, P, Si, and O	Nano needle-like HA	28 ± 5 nm (width) by 160 ± 30 nm (length)	391 – 1,026 nm
S3	*Powder formula* (67 mgCa; 38 mgP; 1.5 mgFe)	Ca, P, and O	Nano needle-like HA	28 ± 7 nm (width) by 237 ± 119 nm (length)	211 – 1,722 nm
S4	*Powder formula* (82 mgCa; 110 mgP; 1.9 mgFe)	Si, O, Ca, P, and K	Nano SiO_2	Spherical diameter: 7 ± 1 nm	None
S5	*Powder formula* (72 mgCa; 40 mgP; 1.5 mgFe)	Ca, P Ti, Al, Si, S, K,	Spherical nano Ca, P *unknown*	30 – 35 nm 10 – 30 nm	1000 – 2000 nm 1000 – 2000 nm
S6	*Liquid Formula* (78 mgCa; NA mgP; 1.8 mgFe)	Ca, O	Nano TiO_2 Nano Ca, O particles	16 – 530 nm 590 ± 126 nm	None 1,184 – 2,647 nm
R1	Hydroxyapatite reference (American Elements Inc.)	Ca, P, O	Nano needle-like HA	30 ± 5 nm (width) by 131 ± 25 nm (length)	141 – 1,786 nm
R2	Hydroxyapatite reference (Chinese supplier)	Ca, P, O	Nano needle-like HA	30 ± 6 nm (width) by 126 ± 28 nm (length)	220 – 1,322 nm
R3	Hydroxyapatite dietary supplement (NOW, Australia)	Ca, P, O	Spherical HA	Diameter: 20 ± 5 nm	225 – 837 nm

392

393

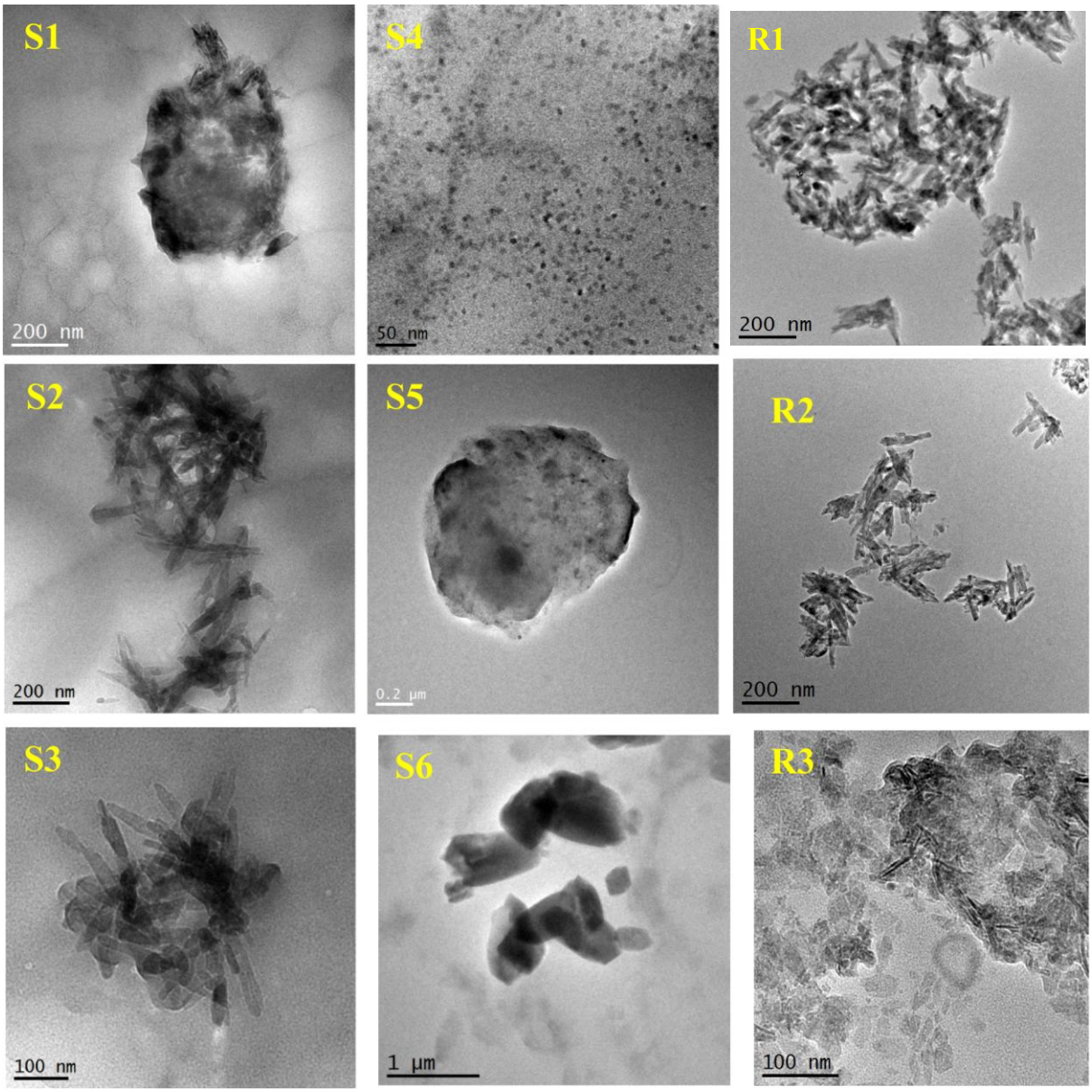

394

395 **Figure 1** – Transmission electron micrographs of particles separated from infant formulas (S1-

396 S6) and reference samples (R1-R3). EDS results summarized in Table 1.

397

398

399

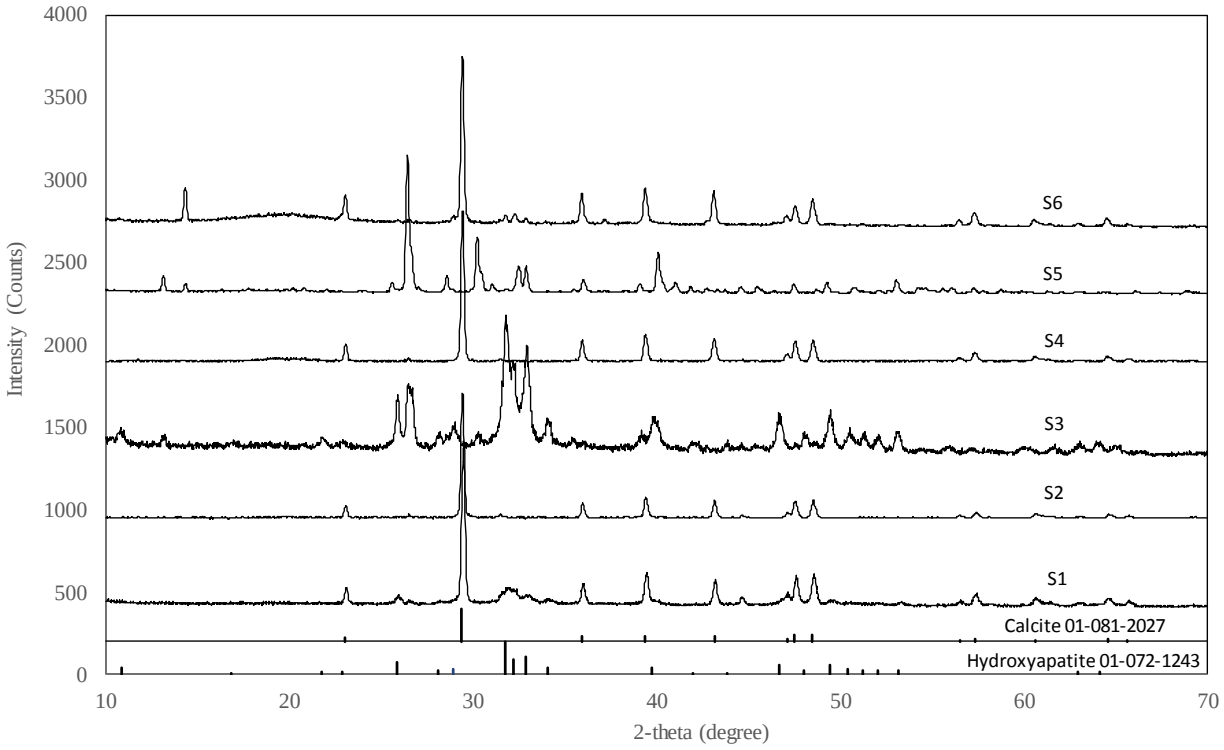

400

401 **Figure 2.** X-ray diffraction patterns of dominant mineral content separated from the six infant

402 formula products and reference XRD patterns for calcite and hydroxyapatite.

403

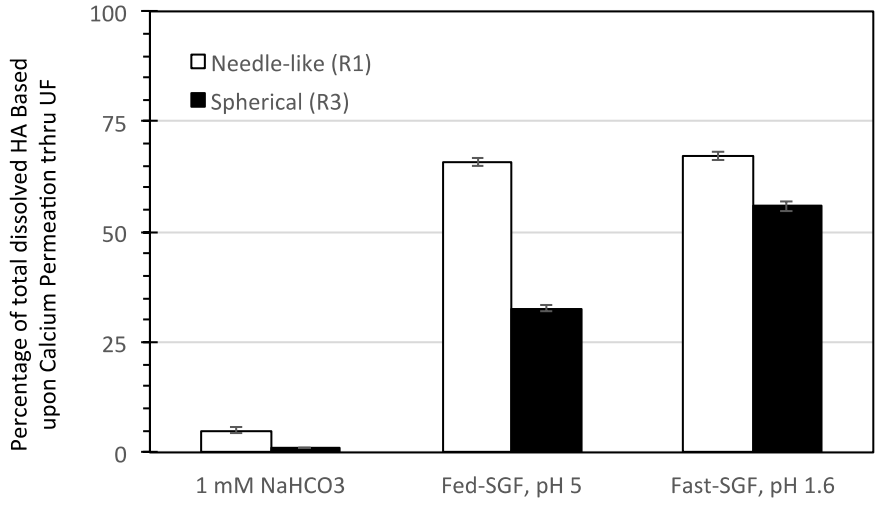

404

405

406 **Figure 3.** Percentage of total dissolved hydroxyapatite in the three simulated fluids based upon

407 percentage of calcium in the ultrafilter permeate relative to the added mass (100 mg HA/L and

408 measured by ICP-MS) present as calcium.

409

REFERENCES

1. Kiser, M.A., et al., *Biosorption of nanoparticles to heterotrophic wastewater biomass.* Water Research, 2010. **44**(14): p. 4105-4114.
2. Kiser, M.A., et al., *Titanium Nanomaterial Removal and Release from Wastewater Treatment Plants.* Environmental Science & Technology, 2009. **43**(17): p. 6757-6763.
3. Keller, A.A. and A. Lazareva, *Predicted releases of engineered nanomaterials:From global to regional to local.* Environ. Sci. Tech. Letters, 2014. **1**(1): p. 65-70.
4. Mueller, N.C. and B. Nowack, *Exposure modeling of engineered nanoparticles in the environment.* Environmental Science & Technology, 2008. **42**(12): p. 4447-4453.
5. Piccinno, F., et al., *Industrial production quantities and uses of ten engineered nanomaterials in Europe and the world.* Journal of Nanoparticle Research, 2012. **14**(9).
6. Gottschalk, F., T. Sun, and B. Nowack, *Environmental concentrations of engineered nanomaterials: Review of modeling and analytical studies.* Environmental Pollution, 2013. **181**: p. 287-300.
7. Reed, R.B., et al., *Solubility of nano-zinc oxide in environmentally and biologically important matrices.* Environmental Toxicology and Chemistry, 2012. **31**(1): p. 93-99.
8. Robichaud, C.O., et al., *Estimates of Upper Bounds and Trends in Nano-TiO2 Production As a Basis for Exposure Assessment* Environ. Sci. Technol., 2009. **43**(12): p. 4227-4233.
9. Kaegi, R., et al., *Fate and transformation of silver nanoparticles in urban wastewater systems.* Water Research, 2013. **47**(12): p. 3866-3877.
10. Thalmann, B., et al., *Sulfidation Kinetics of Silver Nanoparticles Reacted with Metal Sulfides.* Environmental Science & Technology, 2014. **48**(9): p. 4885-4892.
11. Conway, J.R., et al., *Aggregation, Dissolution, and Transformation of Copper Nanoparticles in Natural Waters.* Environmental Science & Technology, 2015. **49**(5): p. 2749-2756.
12. Hong, J., et al., *Toxic effects of copper-based nanoparticles or compounds to lettuce (Lactuca sativa) and alfalfa (Medicago sativa).* Environmental Science-Processes & Impacts, 2015. **17**(1): p. 177-185.
13. Lenton, S., et al., *A review of the biology of calcium phosphate sequestration with special reference to milk.* Dairy Science & Technology, 2015. **95**(1): p. 3-14.
14. Miretzky, P. and A. Fernandez-Cirelli, *Phosphates for Pb immobilization in soils: a review.* Environmental Chemistry Letters, 2008. **6**(3): p. 121-133.
15. Piccoli, P. and P. Candela, *Apatite in Felsic Rocks - A Model for the estimation of initial halogen concentrations in the Bishop Tuff (Long Valley) and Tuolumine Intrusive Suite (Sierra-Nevada Baltholith) magmas* American Journal of Science, 1994. **294**(1): p. 92-135.
16. Vance, M.E., et al., *Nanotechnology in the real world: Redeveloping the nanomaterial consumer products inventory.* Beilstein Journal of Nanotechnology, 2015. **6**: p. 1769-1780.

17. de-Bashan, L.E. and Y. Bashan, *Recent advances in removing phosphorus from wastewater and its future use as fertilizer (1997-2003).* Water Research, 2004. **38**(19): p. 4222-4246.
18. Wiesner, M.R., et al., *Meditations on the Ubiquity and Mutability of Nano-Sized Materials in the Environment.* Acs Nano, 2011. **5**(11): p. 8466-8470.
19. Boisson, J., et al., *Evaluation of hydroxyapatite as a metal immobilizing soil additive for the remediation of polluted soils. Part 1. Influence of hydroxyapatite on metal exchangeability in soil, plant growth and plant metal accumulation.* Environmental Pollution, 1999. **104**(2): p. 225-233.
20. Fuller, C.C., et al., *Mechanisms of uranium interactions with hydroxyapatite: Implications for groundwater remediation.* 2002. **36**(2): p. 158-165.
21. Fan, X., D.J. Parker, and M.D. Smith, *Adsorption kinetics of fluoride on low cost materials.* Water Research, 2003. **37**(20): p. 4929-4937.
22. Straub, D.A., *Calcium supplementation in clinical practice: a review of forms, doses, and indications.* Nutrition in Clinical Practice, 2007. **22**(3): p. 286-296.
23. Ruegsegger, P., A. Keller, and M.A. Dambacher, *Comparison of the treatment effects of Ossein-Hydroxyapatite compound and calcium carbonate in osteoporotic females.* Osteoporosis International, 1995. **5**(1): p. 30-34.
24. SCCS, *Opinion on Hydroxyapatite (nano)*. 2015, European Union Scientific Committee on Consumer Safety: Luxembourg. p. 55.
25. Yang, Y., et al., *Characterization of Food-Grade Titanium Dioxide: The Presence of Nanosized Particles.* Environmental Science & Technology, 2014. **48**(11): p. 6391-6400.
26. Yang, Y., et al., *Survey of food-grade silica dioxide nanomaterial occurrence, characterization, human gut impacts and fate across its lifecycle.* Science of the Total Environment, 2016. **565**: p. 902-912.
27. Marques, M.R.C., R. Loebenberg, and M. Almukainzi, *Simulated Biological Fluids with Possible Application in Dissolution Testing.* Dissolution Technologies, 2011. **18**(3): p. 15-28.
28. Singh, G., et al., *Measurement Methods to Detect, Characterize, and Quantify Engineered Nanomaterials in Foods.* Comprehensive Reviews in Food Science and Food Safety, 2014. **13**(4): p. 693-704.
29. Szakal, C., et al., *Measurement of Nanomaterials in Foods: Integrative Consideration of Challenges and Future Prospects.* Acs Nano, 2014. **8**(4): p. 3128-3135.
30. Yada, R.Y., et al., *Engineered Nanoscale Food Ingredients: Evaluation of Current Knowledge on Material Characteristics Relevant to Uptake from the Gastrointestinal Tract.* Comprehensive Reviews in Food Science and Food Safety, 2014. **13**(4): p. 730-744.
31. Ennos, A.E., *The origin of specimen contamination in the electron microscope.* British Journal of Applied Physics, 1953. **4**(4): p. 101-106.
32. Yang, Y., et al., *Survey of food-grade silica dioxide nanomaterial occurrence, characterization, human gut impacts and fate across its lifecycle.* Science of the Total Environment, in-press (2016).

33. Weir, A., et al., *Titanium Dioxide Nanoparticles in Food and Personal Care Products.* Environ. Sci. Tech., 2012. **46**(4): p. 2242-2250.
34. Yang, Y., et al., *Characterization of Food-Grade Titanium Dioxide: The Presence of Nanosized Particles.* Environmental Science & Technology, 2014. **48**(11): p. 6391-6400.
35. Zhang, Y., et al., *Synthesis of nanorod and needle-like hydroxyapatite crystal and role of pH adjustment.* Journal of Crystal Growth, 2009. **311**(23-24): p. 4740-4746.
36. Sadat-Shojai, M., et al., *Synthesis methods for nanosized hydroxyapatite with diverse structures.* Acta Biomaterialia, 2013. **9**(8): p. 7591-7621.
37. Cao, L.Y., C.B. Zhang, and H.F. Huang, *Synthesis of hydroxyapatite nanoparticles in ultrasonic precipitation.* Ceramics International, 2005. **31**(8): p. 1041-1044.
38. Cornelis, G., et al., *Retention and Dissolution of Engineered Silver Nanoparticles in Natural Soils.* Soil Science Society of America Journal, 2012. **76**(3): p. 891-902.
39. Zhang, W., et al., *Modeling the Primary Size Effects of Citrate-Coated Silver Nanoparticles on Their Ion Release Kinetics.* Environmental Science & Technology, 2011. **45**(10): p. 4422-4428.
40. Li, Y., et al., *Surface-Coating-Dependent Dissolution, Aggregation, and Reactive Oxygen Species (ROS) Generation of Silver Nanoparticles under Different Irradiation Conditions.* Environmental Science & Technology, 2013. **47**(18): p. 10293-10301.
41. Brasiliense, V., et al., *Correlated Electrochemical and Optical Detection Reveals the Chemical Reactivity of Individual Silver Nanoparticles.* Journal of the American Chemical Society, 2016. **138**(10): p. 3478-3483.
42. Erickson, H.P., *Size and Shape of Protein Molecules at the Nanometer Level Determined by Sedimentation, Gel Filtration, and Electron Microscopy.* Biological Procedures Online, 2009. **11**(1): p. 32-51.
43. Montano, M.D., et al., *Improvements in the detection and characterization of engineered nanoparticles using spICP-MS with microsecond dwell times.* Environmental Science-Nano, 2014. **1**(4): p. 338-346.
44. Bi, X.Y., et al., *Quantitative resolution of nanoparticle sizes using single particle inductively coupled plasma mass spectrometry with the K-means clustering algorithm.* Journal of Analytical Atomic Spectrometry, 2014. **29**(9): p. 1630-1639.
45. Pace, H.E., et al., *Single Particle Inductively Coupled Plasma-Mass Spectrometry: A Performance Evaluation and Method Comparison in the Determination of Nanoparticle Size.* Environmental Science & Technology, 2012. **46**(22): p. 12272-12280.
46. Hassellov, M., et al., *Nanoparticle analysis and characterization methodologies in environmental risk assessment of engineered nanoparticles.* Ecotoxicology, 2008. **17**(5): p. 344-361.
47. Arvidsson, R., et al., *Challenges in Exposure Modeling of Nanoparticles in Aquatic Environments.* Human and Ecological Risk Assessment, 2011. **17**(1): p. 245-262.
48. Cwiertny, D.M., et al., *Surface chemistry and dissolution of α-FeOOH nanorods and microrods: Environmental implications of size-dependent interactions with oxalate.* Journal of Physical Chemistry C, 2009. **113**(6): p. 2175-2186.

49. Greer, F.R., *Calcium, Phosphorous, and Magnesium - How much is too much for infant formulas.* Journal of Nutrition, 1989. **119**(12): p. 1846-1851.
50. Moy, R.J.D., *Iron fortification of infant formula.* Nutrition Research Reviews, 2000. **13**(2): p. 215-227.
51. Thompkinson, D.K. and S. Kharb, *Aspects of infant food formulation.* Comprehensive Reviews in Food Science and Food Safety, 2007. **6**(4): p. 79-102.
52. Garner, K.L., et al., *Species Sensitivity Distributions for Engineered Nanomaterials.* Environmental Science & Technology, 2015. **49**(9): p. 5753-5759.
53. Keller, A.A., et al., *Global life cycle releases of engineered nanomaterials.* Journal of Nanoparticle Research, 2013. **15**(6).
54. Keller, A.A., et al., *Release of engineered nanomaterials from personal care products throughout their life cycle.* Journal of Nanoparticle Research, 2014. **16**(7): p. 1-10.
55. Kent, G., *Global infant formula: monitoring and regulating the impacts to protect human health.* International Breastfeeding Journal, 2015. **10**.
56. Bronner, F., *Recent developments in intestinal calcium absorption.* Nutrition Reviews, 2009. **67**(3): p. 109.
57. Pansu, D., et al., *Duodenal and ileal calcium absorption in the rat and effects of vitamin D.* The American journal of physiology, 1983. **244**(6): p. G695-700.
58. Jaeger, P. and W.G. Robertson, *Role of dietary intake and intestinal absorption of oxalate in calcium stone formation.* Nephron - Physiology, 2004. **98**(2): p. p64-p71.
59. Pal, A.K., et al., *Linking Exposures of Particles Released From Nano-Enabled Products to Toxicology: An Integrated Methodology for Particle Sampling, Extraction, Dispersion, and Dosing.* Toxicological Sciences, 2015. **146**(2): p. 321-333.
60. Cohen, J.M., G.M. DeLoid, and P. Demokritou, *A critical review of in vitro dosimetry for engineered nanomaterials.* Nanomedicine, 2015. **10**(19): p. 3015-3032.
61. DeLoid, G., et al., *Estimating the effective density of engineered nanomaterials for in vitro dosimetry.* Nature Communications, 2014. **5**.